Structure Determination of the Coincidence Phase of Graphene on Ru(0001)

W. Moritz,[1,*] B. Wang,[2] M.-L. Bocquet,[2] T. Brugger,[3] T. Greber,[3] J. Wintterlin,[4] and S. Günther[4]

[1]*Department für Geo- und Umweltwissenschaften, Ludwig-Maximilians-Universität München, Theresienstr. 41, 80333 Munich, Germany*

[2]*Université de Lyon, Laboratoire de Chimie, Ecole Normale Supérieure de Lyon, CNRS, France*

[3]*Physik-Institut, University of Zürich, Winterthurerstrasse 190, CH-8057 Zürich, Switzerland*

[4]*Department Chemie, Ludwig-Maximilians-Universität München, Butenandtstr. 11, 81377 Munich, Germany*

(Received 31 August 2009; published 2 April 2010)

The structure of the commensurate (23×23) phase of graphene on Ru(0001) has been analyzed by quantitative low-energy electron diffraction (LEED)-$I(V)$ analysis and density-functional theory calculations. The $I(V)$ analysis uses Fourier components as fitting parameters to determine the vertical corrugation and the lateral relaxation of graphene and the top Ru layers. Graphene is shown to be strongly corrugated by 1.5 Å with a minimum C-Ru distance of 2.1 Å. Additionally, lateral displacements of C atoms and a significant buckling in the underlying Ru layers are observed, indicative for strong local C-Ru interactions.

DOI: 10.1103/PhysRevLett.104.136102 PACS numbers: 68.35.B−, 61.05.J−, 68.43.−h, 71.15.Mb

Graphene can experience massive changes of its properties when put on a metal surface. Depending on the metal the special electronic structure of freestanding graphene near E_F can be modified to a large or minor degree [1–4] and the lattice vibrations can be affected [5]. Interactions with metals are important for the lead contacts in possible graphene-based electronic devices [6], the interactions may be used to control the electronic properties of graphene, and they determine the epitaxial growth of graphene on metals by which extremely well-ordered layers have been prepared [7–10]. There is currently no simple, generally accepted picture of metal-graphene interactions that is able to explain all of the observed effects, such as the strong variations between different metals [11,12]. An important reason is the almost complete lack of experimental structure information—graphene layers on metals generally form incommensurate or long-wave coincidence structures for which structure analyses are exceedingly difficult. Unclear points are, in particular, the metal-graphene separation and the deformations of the graphene layers, which may even depend on the size of the graphene islands [13]. Graphene on Ni(111) is an exception as it forms a (1×1) structure, and a low-energy electron diffraction (LEED) $I(V)$ analysis exists [14]. However, because of the (1×1) structure, the geometry obtained cannot be transferred to the other systems. There is also an early LEED $I(V)$ analysis of an incommensurate graphene overlayer on Pt(111) [15] but it considered perfectly flat graphene and could thus not tell anything about a possible buckling. A recent surface x-ray diffraction (SXRD) analysis of Ru(0001)/graphene showed that the commensurate (23×23) superstructure is connected with lateral displacements in the Ru layers below the graphene sheet [16]. Here we present the structural results of a LEED $I(V)$ analysis and of a new precise density-functional theory (DFT) calculation of graphene on Ru(0001). LEED structure analyses of this size—the considered (13×13)graphene-on-(12×12)Ru structure involved 338 C atoms per unit cell and 432 Ru atoms from the three relaxed Ru layers—have not been performed before. The structure obtained is partially unexpected. To verify it we have therefore additionally performed a precise DFT analysis.

The graphene layers were prepared by thermal decomposition of C_2H_4 on a Ru(0001) surface. The sample was cleaned by Ar^+ sputtering, oxidation and annealing cycles as described earlier [17]. Then 30 L ($1\,\mathrm{L} = 1 \times 10^{-6}$ Torr s) of C_2H_4 were adsorbed at a sample temperature of 1100 K, which led to epitaxial monolayers of graphene. LEED data taken thereafter showed hexagonal patterns with satellites around the substrate spots [Fig. 1(a)]. The satellites are caused by the (25×25)graphene-on-(23×23)Ru coincidence structure. We mention that only every other satellite spot of the superstructure is visible in the diffraction pattern. The reason is that the superstructure unit cell consists of four almost identical subunits, corresponding to a quasiperiodic (12.5×12.5)graphene-on-(11.5×11.5)Ru structure [16]. In the structure model [Fig. 1(b)] one can see the subunits by the twofold periodic height modulation of the graphene layer within one unit cell of the full superstructure. The Fourier components from these subunits completely dominate the diffraction intensity. Also the 30 Å moiré-like structure resolved by scanning tunneling microscopy (STM) is caused by the quasiperiodic subunits [17]. The LEED and DFT structure analyses could therefore be reduced to a smaller unit cell by marginally adjusting the lattice constant to a periodic structure. We chose a (13×13)graphene-on-(12×12)Ru structure; tests on the alternative (12×12)graphene-on-(11×11)Ru structure only gave negligible differences.

DFT calculations were performed with the VASP package, which implements PAW pseudopotentials and the PBE

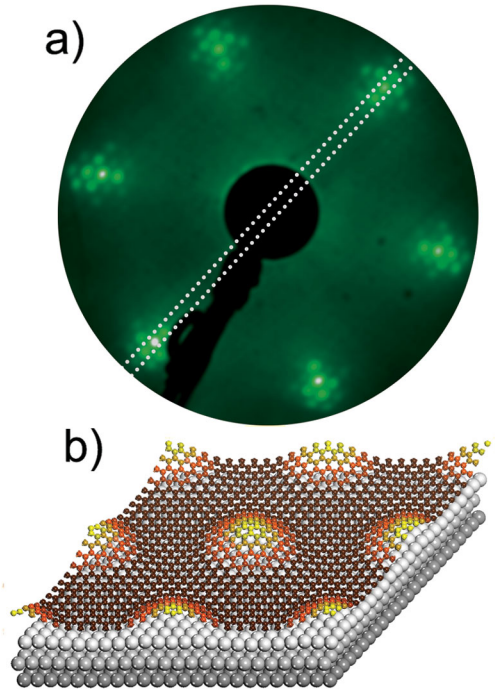

FIG. 1 (color). (a) Leed pattern of graphene on Ru(0001) at 112 eV. (b) 3D structure model of the unit cell. For better visibility, the vertical displacements of the C and Ru atoms are enhanced by factors of 3 and 7, respectively.

exchange correlation functional [18] in the generalized gradient approximation [19]. To enable a detailed comparison with the LEED result a greater precision than in a previous study was chosen [20]. The slabs consisted of one graphene layer and four Ru layers, with two Ru layers relaxed, and a vacuum region of 10.5 Å. Because of the large cell, the 2D Brillouin zone was sampled with a single k point. The cutoff energy was set at 400 eV, the convergence criterion was an atomic force of 30 meV/Å. The lateral Ru lattice constant was set to 2.724 Å, the optimized value for bulk crystalline Ru. The lattice constant of the freestanding graphene was adjusted accordingly.

LEED $I(V)$ curves were recorded in the energy range between 60 and 240 eV using a backview OMICRON SPECTALEED. Full LEED patterns were recorded in 2 eV steps on a CCD video camera (SBIG ST-7) [21]. Because of the difficulty of the close spacings between the satellite spots, 1D profiles were taken along stripes connecting the centers of the respective peaks, as indicated in Fig. 1(a). The peak intensities were extracted by fitting Voigt functions to the peaks and subtracting a linear background. The diffraction pattern exhibits the $p3m1$ symmetry of the substrate and the $I(V)$ curves were averaged accordingly.

LEED calculations were restricted to models with $p3m1$ symmetry. The beam set neglect method was used [22]. Convergence was checked by comparison with a full calculation for one model. The phase shifts were calculated from a superposition of atomic potentials using optimized muffin-tin radii [23]. Nine phase shifts were used. A least-squares scheme was used to optimize the structural and thermal parameters in the graphene and top three substrate layers [24]. To reduce the number of free parameters, the modulation was described by Fourier coefficients limited to the third order. Higher-order Fourier coefficients did not improve the final agreement. For the lateral shifts in the graphene layer, the Fourier coefficients derived from the DFT result were used as start parameters. Overall 60 independent Fourier components for lateral and vertical modulations in the graphene layer and in three substrate layers were optimized together with 4 interlayer distances. In the final analysis anisotropic thermal displacements in the C layer were considered using the multipole expansion for the probability density [25]. A very shallow minimum was found for an rms displacement of 0.04 Å lateral and 0.08 Å normal to the surface neglecting a possible difference in low and high regions in the graphene layer. In the Ru layers only isotropic displacements were assumed. The r factor for the best fit model was $r_P = 0.29$, the comparison with the experimental curves is shown in Fig. 2.

We mention that an independent SXRD analysis that has been submitted for publication reports chiral lateral displacements in the graphene layer [26]. The resulting reduced $p3$ symmetry is beyond what the present, already huge LEED structure analysis could treat. The symmetry reduction therefore cannot be excluded from the LEED results. Otherwise, the x-ray results are very similar though a smaller corrugation of the graphene layer was found and a different corrugation of the Ru layer.

The main features of the structure model obtained by LEED are a minimum metal-graphene separation of only 2.1 Å and a considerable buckling of the graphene layer of 1.53 ± 0.2 Å [Fig. 3(a)]. The values from DFT, 2.2 Å for the minimum distance and 1.59 Å for the buckling are almost the same. For the (12×12)graphene-on-(11×11)Ru structure the corresponding values from DFT are 2.1 and 1.5 Å, proving that these data are robust with respect to small changes of the unit cell. For LEED the results for a (11×11) unit cell change much less than the error limits.

The actual (23×23) structure should thus be well captured, and is very similar to a further recent DFT study of Ru(0001)/graphene [27]. The graphene-metal layer distance compares also well to Ni(111)/graphene for which values between 2.11 and 2.16 Å were found [14]. The same values occur in the adsorbate system benzene/Ru(0001) [28]. The relaxations (error bars 0.04 Å) of the Ru layer spacings [Fig. 3(a)] remain nearly unchanged with respect to the uncovered surface [29]. Both from LEED and DFT the maxima of the buckled layer correspond to configurations where the two carbon atoms of the graphene unit cell occupy the two hollow sites, i.e., the (hcp, fcc) positions. At the minima the carbon atoms alternately occupy top and hollow sites, resulting in (fcc, top) or (top, hcp) configurations. The height difference between these two minima is

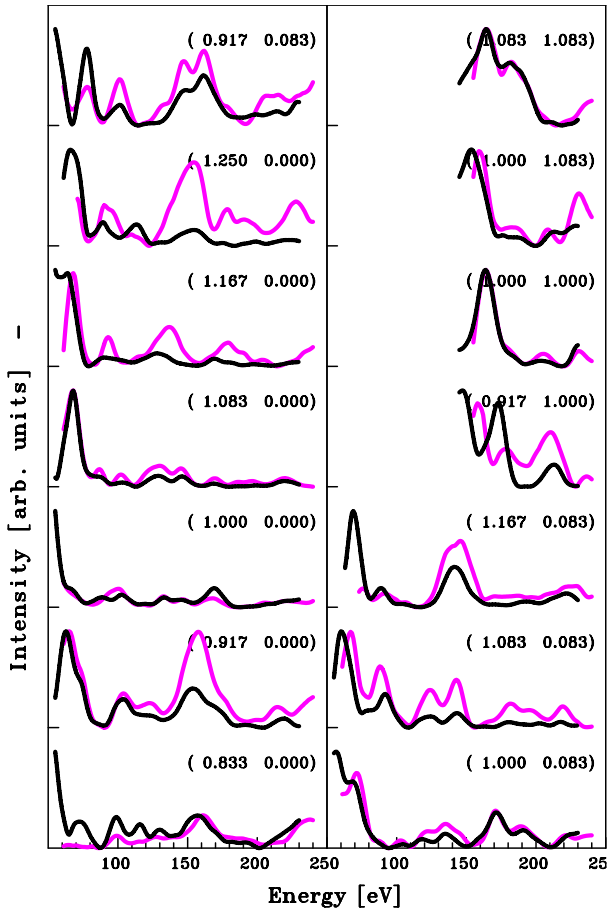

FIG. 2 (color online). Experimental (red [gray]) and calculated (black) $I(V)$ curves for the best fit model.

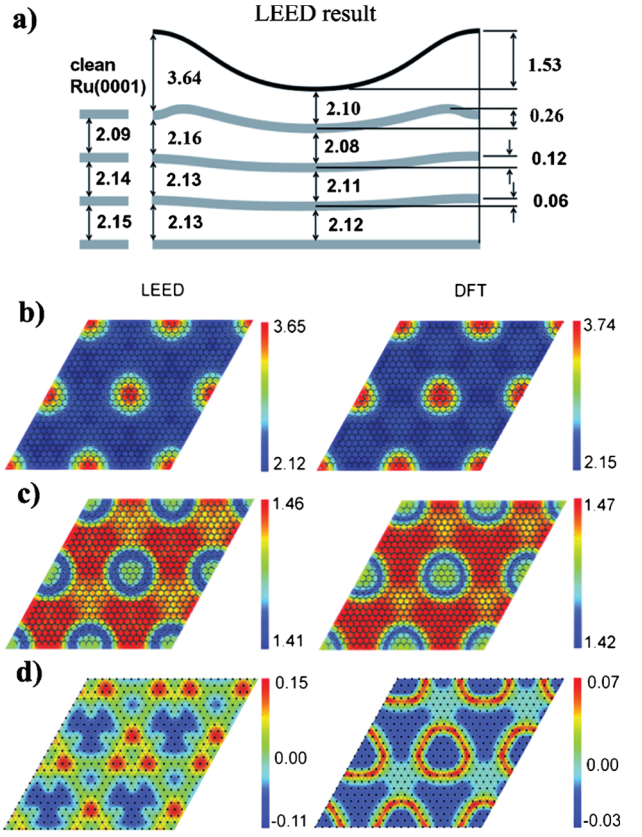

FIG. 3 (color). Corrugations determined by DFT and LEED. (a) Vertical distances at the maxima and minima from LEED (schematically, lateral directions are not included); numbers in Å. (b) Corrugation of the graphene layer (c) Variation of bond lengths in the graphene layer (d) Corrugation of the topmost Ru layer.

0.03 Å (LEED) and about 0.08 Å (DFT). A possible height difference between neighboring C atoms in the graphene layer was investigated, but was below the error limits of LEED and below 0.03 Å in the low region in DFT. The adsorbed graphene layer thus remains sp^2 hybridized. These results resolve conflicting reports about the structure of epitaxial graphene on Ru(0001) [30,31].

The corrugation of the graphene layer of 1.5 Å is larger than the value from the current SXRD analysis (1.0 Å [26]. The reason for this discrepancy, which is outside the error bars of both studies, could not yet be resolved, though might be related to the mirror symmetry breaking as proposed by Martoccia *et al.* [26]. A recently proposed model with additional Ru atoms underneath the hills in the graphene layer [32] requiring a corrugation amplitude of about 2 Å led to r factors above 0.46 and seems to be unlikely. Corrugation amplitudes of the order of 1 Å were measured by STM [17] and obtained in a previous DFT study [20], whereas He scattering and scanning tunneling spectroscopy data indicated a much weaker height modulation [33]. A small corrugation would be consistent with the van der Waals-type interaction expected for metal-graphene systems that would lead to a large metal-graphene spacing. Such a situation was actually found by DFT [34] for Ir/graphene. For Ru(0001) the structure obtained rules out such a picture. The spacing strongly oscillates between typical van der Waals distances—the layer distance in graphite is 3.35 Å—and much shorter distances where the bonding type must be qualitatively different (despite the intact sp^2 hybridization). These strongly interacting areas provide an explanation for the massive changes in the π/π^* electronic band structure of graphene, in particular, a band gap of more than 4 eV below E_F [2,4]. That Ru and Ir may actually be different in this respect was also indicated by core-level spectroscopy [11].

Important second order effects are a variation of bond lengths in the graphene sheet [Fig. 3(c)] and a buckling of the topmost layer of Ru atoms [Fig. 3(d)]. Lateral relaxation in the graphene sheet reduced the r factor significantly from 0.34 to 0.29, a slightly smaller influence had the buckling in the top Ru layer. Further relaxations in deeper layers were found below the error limits at the present level of agreement. Overall the C-C bond length is stretched by 0.015 Å for the (12×12)-Ru unit cell compared to the true (23×23) unit cell. At the corrugation maxima the C-C bonds are 0.012 Å shorter than this average value, at the minima they are 0.018 Å longer (from LEED). DFT finds

the same trends, values are 0.010 Å and 0.016 Å. These horizontal distortions agree with the above bonding picture. At the corrugation maxima, where the graphene hardly interacts (there may be even a repulsion), the bond lengths are the same as for freestanding graphene. At the corrugation minima the bonds are stretched, indicating weaker C-C bonds, which is caused by the interactions of these atoms with the metal. The buckling of the first Ru layer amounts to 0.26 and 0.10 Å from LEED and DFT, respectively. The small DFT buckling might be related to the fact that the DFT calculations did only allow relaxations in 2 layers. A buckling down to the third Ru layer was considered in LEED, while the XRD [26] shows that the substrate relaxation goes as deep as 7 layers which underpins the substantial chemical effect of the graphene layer. In detail, the buckling of the first Ru layer is complex [Fig. 3(d)]. The strongest outward relaxation does not occur at the graphene minima but in areas (triangular in LEED, ringlike in DFT) around the maxima. A possible explanation is that the strongly interacting regions are more extended than the areas where local (fcc, top) and (top, hcp) bonding configurations are present. The height maxima of the graphene layer are surrounded by a zone, where C atoms in local bridge positions are found. For graphene on Ni(111) such bridge positions were found to be favorable [35]. Similarly, for graphene on Ru(0001) DFT calculations showed that these bridge type configurations are energetically favorable. Thus, we can also expect relatively strong C-Ru interactions in these ''bridge-bonded'' zones. Because the graphene layer is stiffer than the Ru layer the Ru atoms at these transition regions between the strongly and weakly interacting regions are pulled up. We propose therefore that the effect results from an interplay between local chemical Ru-C bonds and the elastic properties of the graphene and the metal.

The combined LEED $I(V)$ and DFT study clearly evidences a large height corrugation of about 1.5 Å of graphene on Ru(0001) with a minimum graphene-Ru layer distance of 2.1 Å. The unit cell consists of areas with strongly interacting C atoms, which are close to the Ru substrate, and areas with weakly interacting C atoms, which are at larger distances from the Ru substrate and occupy (hcp, fcc) hollow sites. This separation into weakly and strongly bound areas is supported by the lateral variation of the local C-C bond length, as found by DFT and LEED. The distortions in the Ru layer are more complex and probably involve the interplay of chemical bonding and elastic properties of the graphene layer. The solved structure of graphene on Ru(0001) explains many properties of this system, which may be an ideal candidate as a template for macromolecules or clusters.

We acknowledge support by the German Science Foundation (PE883/1-2) and a grant for computational time at the Leibniz Rechenzentrum Garching. B. W. acknowledges support by the European Commission through the Early Stage Researcher Training Network MONET, MEST-CT-2005-020908.

*w.Moritz@lrz.uni-muenchen.de

[1] A. Nagashima, N. Tejima, and C. Oshima, Phys. Rev. B **50**, 17 487 (1994).
[2] T. Brugger *et al.*, Phys. Rev. B **79**, 045407 (2009).
[3] I. Pletikosic *et al.*, Phys. Rev. Lett. **102**, 056808 (2009).
[4] P. Sutter, M. S. Hybertsen, J. T. Sadowski, and E. Sutter, Nano Lett. **9**, 2654 (2009).
[5] C. Oshima and A. Nagashima, J. Phys. Condens. Matter **9**, 1 (1997).
[6] B. Huard, N. Stander, J. A. Sulpizio, and G. Goldhaber-Gordon, Phys. Rev. B **78**, 121402(R) (2008).
[7] P. W. Sutter, J.-I. Flege, and E. A. Sutter, Nature Mater. **7**, 406 (2008).
[8] R. van Gastel *et al.*, Appl. Phys. Lett. **95**, 121901 (2009).
[9] Y. Pan *et al.*, Adv. Mater. **21**, 2777 (2009).
[10] E. Loginova, N. C. Bartelt, P. J. Feibelman, and K. F. McCarty, New J. Phys. **11**, 063046 (2009).
[11] A. B. Preobrajenski, M. L. Ng, A. S. Vinogradov, and N. Mårtensson, Phys. Rev. B **78**, 073401 (2008).
[12] J. Wintterlin and M. L. Bocquet, Surf. Sci. **603**, 1841 (2009).
[13] P. Lacovig *et al.*, Phys. Rev. Lett. **103**, 166101 (2009).
[14] Y. Gamo, A. Nagashima, M. Wakabayashi, M. Terai, and C. Oshima, Surf. Sci. **374**, 61 (1997).
[15] Z.-P. Hu, D. F. Ogletree, M. A. Van Hove, and G. A. Somorjai, Surf. Sci. **180**, 433 (1987).
[16] D. Martoccia *et al.*, Phys. Rev. Lett. **101**, 126102 (2008).
[17] S. Marchini, S. Günther, and J. Wintterlin, Phys. Rev. B **76**, 075429 (2007).
[18] J. P. Perdew, K. Burke, and M. Ernzerhof, Phys. Rev. Lett. **77**, 3865 (1996).
[19] G. Kresse and D. Joubert, Phys. Rev. B **59**, 1758 (1999).
[20] B. Wang, M.-L. Bocquet, S. Marchini, S. Günther, and J. Wintterlin, Phys. Chem. Chem. Phys. **10**, 3530 (2008).
[21] T. Greber,O. Raetzo, T. J. Kreutz, P. Schwaller, W. Deichmann, E. Wetli, and J. Osterwalder, Rev. Sci. Instrum. **68**, 4549 (1997).
[22] M. A. Van Hove, Rongfu Lin, and G. A. Somorjai, Phys. Rev. Lett. **51**, 778 (1983).
[23] J. Rundgren, Phys. Rev. B **68**, 125405 (2003).
[24] H. Over, U. Ketterl, W. Moritz, and G. Ertl, Phys. Rev. B **46**, 15 438 (1992).
[25] J. Landskron and W. Moritz, Surf. Sci. **337**, 278 (1995).
[26] D. Martoccia *et al.*, arXiv:0908.4517.
[27] D. Jiang, M. Du, and S. Dai, J. Chem. Phys. **130**, 074705 (2009).
[28] G. Held, W. Braun, H.-P. Steinrück, S. Yamagishi, S. J. Jenkins, and D. A. King, Phys. Rev. Lett. **87**, 216102 (2001).
[29] A. P. Baddorf, V. Jahns, D. M. Zehner, H. Zajonz, and D. Gibbs, Surf. Sci. **498**, 74 (2002).
[30] B. Wang, M.-L. Bocquet, S. Günther, and J. Wintterlin, Phys. Rev. Lett. **101**, 099703 (2008).
[31] A. L. Vázquez de Parga *et al.*, Phys. Rev. Lett. **101**, 099704 (2008).
[32] E. Starodub *et al.*, Phys. Rev. B **80**, 235422 (2009).
[33] A. L. Vázquez de Parga *et al.*, Phys. Rev. Lett. **100**, 056807 (2008).
[34] A. N'Diaye, S. Bleikamp, P. J. Feibelman, and T. Michely, Phys. Rev. Lett. **97**, 215501 (2006).
[35] M. Fuentes-Cabrera, M. I. Baskes, A. V. Melechko, and M. L. Simpson, Phys. Rev. B **77**, 035405 (2008).